BMC Oral Health

RESEARCH

Open Access

Relationship between interincisal angles and TMJ morphology/position and trabecular structure: a retrospective study

Xiaowen Hu[1], Ziwei Chen[1], Minhua Mo[1], Xiaohe Zhou[1] and Liangjiao Chen[1*]

Abstract

Background TMJ morphology/position and trabecular structure are influenced by various factors. The role of the interincisal angle, an indicator of the anterior occlusal relationship, on TMJ remains unclear. This study aims to investigate the morphology, trabecular bone structure, and position of the condyle, as well as the glenoid fossa's morphology in skeletal class II populations with different interincisal angles.

Materials and methods A total of 150 adult patients with normodivergent facial types and skeletal class II malocclusions were selected and divided into three groups based on their interincisal angles: normal, small, and large angle groups. The indexes of TMJ were measured using cone-beam computed tomography (CBCT) data and analyzed using Dolphin Imaging, Mimics, and ImageJ.

Results The small angle group had the smallest anteroposterior diameter (APD), while the large angle group had a greater mediolateral diameter (MLD). The large angle group exhibited significantly the largest maximum axial area, bone surface area, and bone volume ($P < 0.05$). Small and large angle groups exhibited greater bone trabeculae (Tb. N) and thinner trabecular thickness (Tb. Th). Compared to the normal angle group, the small angle group exhibited a larger horizontal condylar angle and smaller bilateral condylar angles on the axial plane, while the large angle group showed the opposite trend. Small and large angle groups showed a reduced vertical condyle angle on the coronal plane, with the largest reduction observed in the large angle group ($P < 0.05$). Small and large angle groups had higher heights of the glenoid fossa (GFH). The large angle group exhibited the greatest GFH and width of the glenoid fossa (GFW) ($P < 0.05$).

Conclusion The large angle group had elongated oval and large condyles, and deeper glenoid fossae, while a flattened-oval and smaller condyle, and wider and shallower glenoid fossae were observed in the small angle group. Small and large interincisal angle affects the structure of condylar trabeculae, resulting in thinner Tb. Th and greater Th. N. In the condylar position, small and large angle groups exhibit condylar rotation in the axial and coronal planes. Therefore, the interincisal angle affects the morphology, position, and trabecular structure of the TMJ. This implies that we must pay attention to the impact of the interincisal angle on TMJ, and it is crucial to restore the normal interincisal angle during orthodontic treatment.

*Correspondence:
Liangjiao Chen
2010686017@gzhmu.edu.cn

Full list of author information is available at the end of the article

© The Author(s) 2024. **Open Access** This article is licensed under a Creative Commons Attribution-NonCommercial-NoDerivatives 4.0 International License, which permits any non-commercial use, sharing, distribution and reproduction in any medium or format, as long as you give appropriate credit to the original author(s) and the source, provide a link to the Creative Commons licence, and indicate if you modified the licensed material. You do not have permission under this licence to share adapted material derived from this article or parts of it. The images or other third party material in this article are included in the article's Creative Commons licence, unless indicated otherwise in a credit line to the material. If material is not included in the article's Creative Commons licence and your intended use is not permitted by statutory regulation or exceeds the permitted use, you will need to obtain permission directly from the copyright holder. To view a copy of this licence, visit http://creativecommons.org/licenses/by-nc-nd/4.0/.

Keywords Interincisal angle, Temporomandibular joint, Morphology, Bone trabecula, Occlusion

Background

The temporomandibular joint (TMJ) serves as the functional basis for mandibular movements, including mastication, deglutition, and speech [1]. The morphology and position of the TMJ are influenced by various factors, such as anterior crossbite, and deep bite [2–5]. The anterior occlusion significantly affects the bone mineral density (BMD) of condylar trabeculae [6]. The interincisal angle is the angle between the long axes of the clinical crowns of the upper and lower incisors, which can be easily obtained in a clinic. Angle class II[1] is characterised by a small interincisal angle, while a large interincisal angle in Angle class II[2 [7]]. It is reported that Angle class II[1] exhibited a wider anterior joint space compared to those with Angle class II[2 [8]]. Angle class II [2] have a greater tendency for inward rotation of the condyle [9]. The normal interincisal angle promotes a balanced contraction force of the masticatory muscles, which is beneficial to the TMJ and enables it to withstand occlusal load effectively [10,11]. A large or small interincisal angle may influence the TMJ morphology. It is reported that individuals with large interincisal angles exhibit wider and deeper glenoid fossa compared to small interincisal angles [8]. There are notable variations in condylar position among skeletal Class II malocclusion cases with different vertical facial types [12]. However, the characteristics of the TMJ in Angle Class II with different interincisal angles were unclear. The objective of this study is to investigate the TMJ characteristics in Angle class II samples with normodivergent facial types and focus on the effect of interincisal angles. The null hypothesis posited that there was no statistically significant association between different interincisal angles and the morphological characteristics, trabecular bone structure, condylar position, as well as glenoid fossa morphology in skeletal class II with normodivergent facial types.

1 Materials and methods

Subjects and imaging

The required sample size for this study was determined using PASS15.0 (NCSS, LLC). A test level of $\alpha=0.05$ and a test power of $1-\beta=0.9$ were employed in the calculation, with the predictive value established through preliminary experimentation. Based on these calculations, a total of 138 samples were deemed necessary. In this retrospective study, we collected 150 samples (300 TMJs) from patients who visited the Department of Orthodontics at Stomatological Hospital affiliated with Guangzhou Medical University between January 2019 and June 2021. The average age of the participants was 26.15 (±2.94) years. This study was permitted by the Research Ethics Committee of Stomatological Hospital affiliated with Guangzhou Medical University (No. LCYJ2022019).

The inclusion criteria were as follows: individuals aged between 18 and 35 with a normodivergent facial type (mandibular plane–Frankfurt horizontal angle (MP-FH) ranging from 25.5° to 36.7° [13]), skeletal class II (subspinale-nasion-supramental angle (ANB) > 5°), complete permanent dentition with or without a third molar, good periodontal health, mandibular symmetry (gnathion deviation less than 2 mm) [14], no history of orthodontic treatment, and good general condition. The exclusion criteria were as follows: bad oral habits, open bite, dentition defect, condylar deformity, maxillofacial trauma or orthodontic treatment history, metabolic bone disease, systemic skeletal disease, and systemic disease.

The patients were divided into groups based on the interincisal angle (U1-L1) and the angle between the axis of the upper incisor and the sella-nasion plane (U1-SN). The sample size of each group was 50. The normal angle group was defined as having a normal interincisal angle with 116°≤U1-L1≤132°. The small angle group was defined as having a small interincisal angle with U1-L1 < 116°. Finally, the large angle group was defined as having a large interincisal angle with U1-L1 > 132°.

The patients' initial lateral cephalometric digital films and craniofacial CBCT images were obtained during their orthodontic visit. The lateral cephalometric digital films were taken by ORTHOPHOS XG (Sirona group, Bensheim, Germany) in lateral cephalogram mode. The settings were 73 KV and 15 ma, resulting in an image size of 23 cm×18 cm. The direction of the X-ray projection was from right to left. Craniofacial CBCT images were obtained by the same clinician using newtom vgi (newtom VG, Volumetric scanner, Aperio, Italy) with a slice thickness of 0.3 mm for each axial section. The machine exposure parameters were set to 90.0 kv and 4.0 ma, with a field of view measuring 17 cm×13 cm. During CBCT imaging, patients were positioned upright with their eyes looking straight ahead and their jaws in intercuspal occlusion. The FH planes of the patients were parallel to the ground while their midsagittal plane was perpendicular to it. The lateral cephalometric digital films and CBCT data were analyzed using Dolphin Imaging 11.8 software (Dolphin Imaging & Management Solutions, Chatsworth, CA91311 USA), Mimics 20.0 software (Materialise NV, Leuven, Belgium), and ImageJ software (National Institutes of Health, Bethesda, MD, USA).

Measurements

Dolphin Imaging software was utilized to evaluate the samples' lateral cephalograms. Of note, it was necessary

to mark the subspinale point (A point), nasion point (N point), supramental point (B point), sella point (S point), menton point (Me point), orbitale point (O point), and porion point (P point) and measure the values of MP-FH, ANB, interincisal angle, and U1-SN on the cephalograms to select the sample area (Fig. 1A). In CBCT three-dimensional (3D) reconstruction, chin deviation is assessed by measuring the horizontal distance between pogonion (Pog) and the midsagittal plane (Fig. 1B). The midsagittal line is defined as the line passing through the crista gali and anterior nasal spine points. The FH plane was established as the fundamental plane, with the right orbitale and bilateral porion serving as the reference points for the horizontal orientation. Axial planes were parallel to the FH plane, coronal planes were perpendicular to axial planes, and sagittal planes were perpendicular to coronal and axial planes (Fig. 1C-E).

The CBCT images were imported into Dolphin Imaging software and Mimics 20.0 software to assess the morphology, trabecular bone structure, and position of the condyle as well as the morphology of the glenoid fossa in the maximum axial, coronal and sagittal planes (Figs. 2 and 3) and Table 1 shows the indices. The condyles were measured separately on both sides, with separate measurement planes established for each side. The maximum axial plane of the condyle was determined using the calculation tool in ImageJ. The maximum coronal was defined by the most medial and lateral points of the condyle, and the maximum sagittal planes were defined by the most anterior and posterior points of the condyle in the maximum axial plane. The microstructure

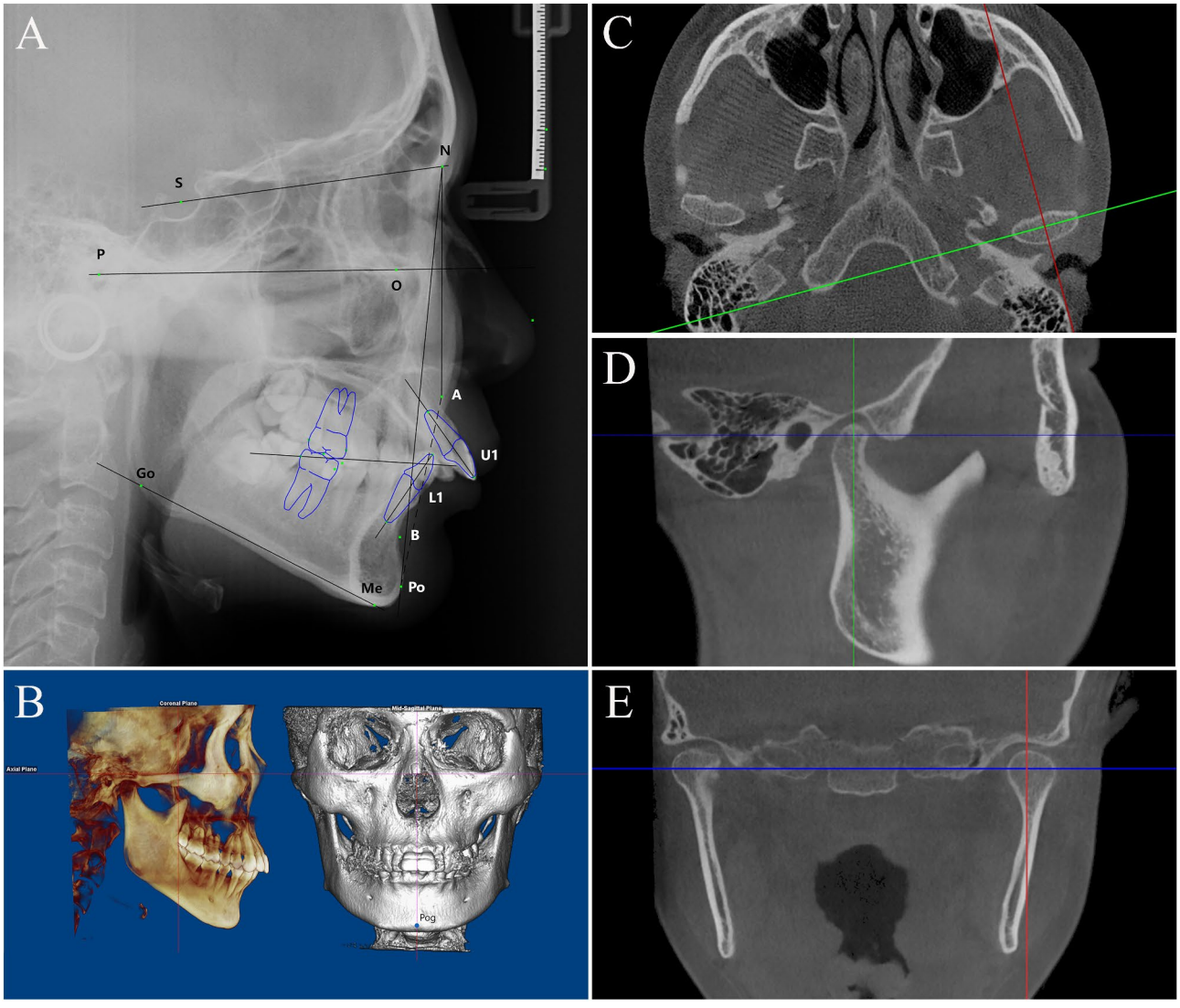

Fig. 1 Cephalometric image and CBCT. (**A**) Landmarks on the lateral cephalogram. (**B**) Setting the Frankfurt (FH) plane and measuring the chin deviation in the 3D reconstruction image of CBCT. Pog, pogonion. Three views of the maximum plane of the condyle on. CBCT: (**C**) maximum axial plane; (**D**) maximum sagittal plane; (**E**) maximum coronal plane

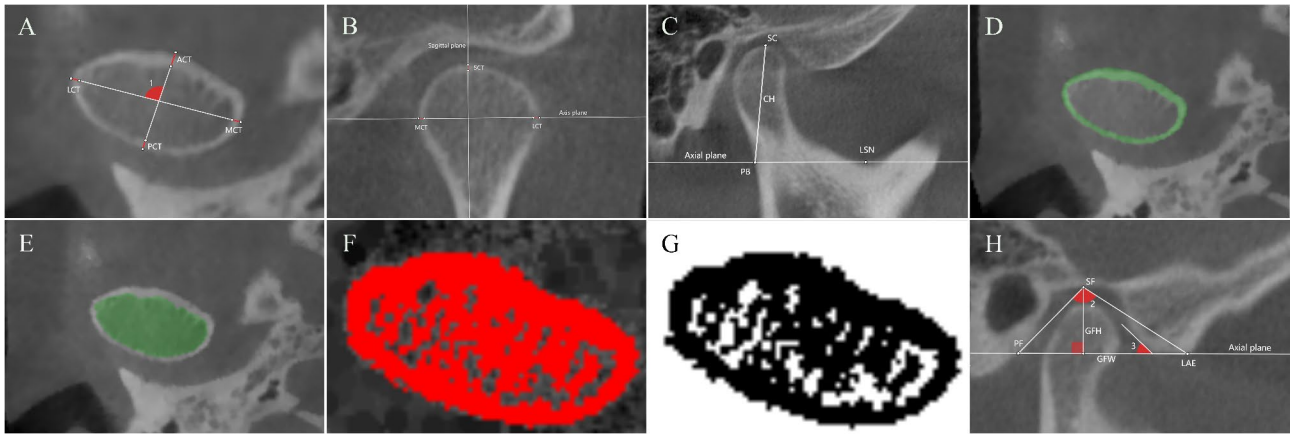

Fig. 2 Measurements of the morphology and trabecular bone structure of the condyle and morphology of the glenoid fossa. (**A**) ∠1, angle of anteroposterior to mediolateral diameter; MCT, medial cortical thickness; LCT, lateral cortical thickness; ACT: anterior cortical thickness; PCT, posterior cortical thickness. (**B**) MCT, medial cortical thickness; SCT, superior cortical thickness; LCT, lateral cortical thickness. (**C**) CH, condylar height; SC, the most superior point of the condyle; LSN, the lowest point of the sigmoid notch; PB, the point of intersection between the tangent line of LSN and the posterior border of the mandibular ramus, the tangent line is parallel to the FH plane. (**D**) and (**E**) Measurement of the area and perimeter of the condylar cortex and cancellous bone. (**F**) Three continuous maximum axial planes of the condyle were selected as measurement areas. (**G**) Image after binarization of the measurement area. (**H**) ∠2, angle of glenoid fossa; ∠3, articular eminence inclination; PF, the tangent line of the lowest point on the articular eminence intersects with the posterior wall of the glenoid fossa, the tangent line is parallel to the FH plane; SF, the most superior point of the glenoid fossa; LAE, the lowest point of the articular eminence; GFH, height of the glenoid fossa; GFW, width of the glenoid fossa

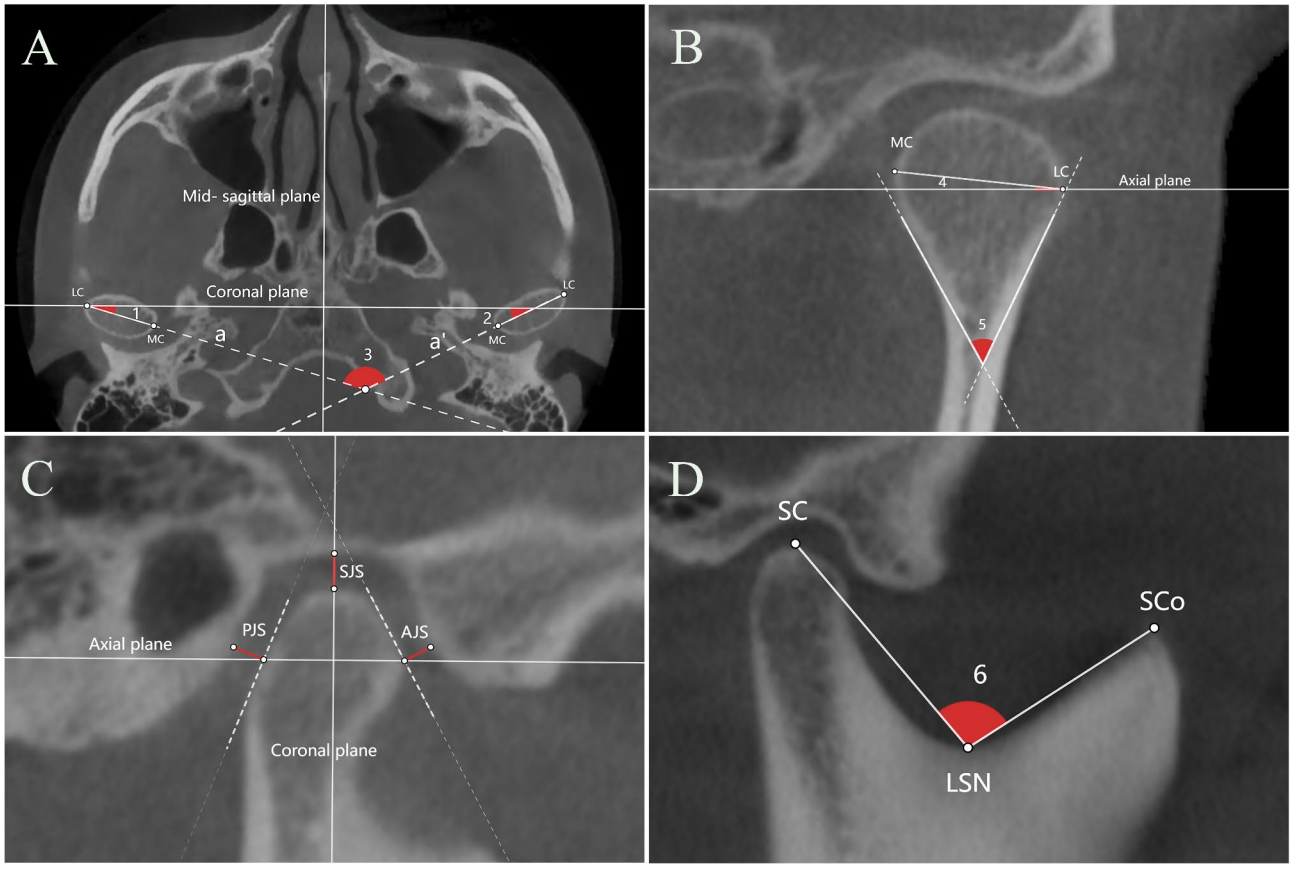

Fig. 3 Landmarks and measurements of condylar position. (**A**) ∠1 and ∠2, the horizontal angle of the condyle; ∠3, the angle of the bilateral condyle. (**B**) ∠4, vertical angle of the condyle; MC, the most medial condylar point; LC, the most lateral condylar point. (**C**) AJS, anterior joint space; SJS, superior joint space; PJS, posterior joint space. (**D**) ∠6, angle of the condyle and coracoid (CCA); SC, the most superior point of the condyle; sco, the most superior point of the coracoid; LSN, the lowest point of the sigmoid notch

Table 1 List of abbreviations and measurements used in the study

Abbreviation	Definition	Measurements
Condylar morphology		
APD	Anteroposterior diameter	Linear distance measured between the most anterior and posterior points of the condyle
MLD	Mediolateral diameter	Linear distance measured between the most medial and lateral points of the condyle
APD/MLD	The ratio of anteroposterior diameter to mediolateral diameter	\
AMA	Angle of anteroposterior diameter to mediolateral diameter	The internal angle between the anteroposterior diameter and mediolateral diameter
MCT	Medial cortical thickness	The thickness of the cortical bone measured at the most anterior, posterior, medial, lateral, and superior points of the condyle on the maximum axial and coronal plane [16]
LCT	Lateral cortical thickness	
ACT	Anterior cortical thickness	
PCT	Posterior cortical thickness	
SCT	Superior cortical thickness	
CH	Condylar height	The linear distance between the SC and PB [17]
Condylar position		
HCA	Horizontal condylar angle	Internal angle between the extended line of MLD and the coronal plane
BCA	Bilateral condylar angle	The internal angle between two extended lines of the MLD of the bilateral condyle
CVA	Vertical condylar angle	The internal angle between the MLD and the axial plane
NCA	Condylar neck angle	The internal angle between two extended lines of the lateral cortical bone of the condylar neck
AJS	Anterior joint space	Closest distance between the most anterior, superior and posterior condylar point and the glenoid fossa wall
SJS	Superior joint space	
PJS	Posterior joint space	
CCA	The angle of the condyle and coracoid	The internal angle from the SC point, LSN point and SCO point[17]
Morphology of the glenoid fossa		
GFW	Width of the glenoid fossa	Distance between LAE and PF
GFH	Height of the glenoid fossa	The perpendicular distance between SF and line LAE-PF
AEI	Articular eminence inclination	Internal angle of the best-fit line of the posterior inclined plane of articular eminence and the FH plane
GFA	Angle of the glenoid fossa	The internal angle between LAE, SF and PF
GFW/GFH	The ratio of the GFW to the GFH	\

of the condylar bone was assessed on the three largest continuous axial sections of the condyle, which were selected based on area calculations conducted in ImageJ (Fig. 2F, G) and the threshold is set to 30–35. The BoneJ2 plugin in ImageJ is utilized for the analysis of the following parameters require measurement: bone superficial area (BS), bone volume (BV), bone-specific surface area (BS/BV), trabecular thickness (Tb.Th), trabecular number (Tb.N) and trabecular separation (Tb.Sp) [15] (The details can be found on the official website called BoneJ (imagej.net).).

All samples underwent duplicate analysis by two researchers within two weeks. Each researcher performed their analysis twice to ensure both intra- and inter-examiner reliability of the selected measurements. The mean value was adopted as the final measurement outcome.

Statistical analysis

Statistical analysis was conducted using SPSS software version 21.0 (IBM, New York, USA). The normality of the data was assessed by the Shapiro-Wilk test, and non-parametric tests were employed for non-normally distributed data. A paired t-test was utilized to compare bilateral condyle indices within each group. Age, sex, MP-FH, ANB and chin deviation were subjected to analysis of variance (ANOVA) for the three groups. The ANOVA was also used to analyze other measurement indices. When comparing between groups, the LSD t-test was used to assess the homogeneity of variance, and Dunnett's T3 test was employed for the heterogeneity of variance. The interincisal angle was subjected to Pearson correlation analysis in relation to condylar morphology, trabecular bone structure, condylar position, and glenoid fossa morphology. The intraclass correlation coefficient (ICC) was used for assessing random errors. The level

of statistical significance was set at $P<0.05$. A post hoc power analysis was conducted using gpower 3.1, with a test level $\alpha=0.05$ and predictive value employed. The calculated power (1-β) was found to be high at 0.953.

Results

For all the analyzed measures, both intra-operator (operator 1: $r=0.974–0.979$; operator 2: $r=0.950–0.982$) and inter-operator ($r=0.768–0.835$) ICCs demonstrated excellent agreement and good reliability. There were no statistically significant differences in the relevant measurements of the left and right TMJ among all the groups ($P>0.05$) (Annexed Tables 1, 2, 3, and 4). There was no significant difference in age, sex, MP-FH, ANB, or chin deviation among the three groups ($P>0.05$) (Annexed Table 1). The data in each group exhibited a normal distribution.

Condylar morphology

The condyle morphology on the maximum axial plane can be classified into three types based on related indexes: oval, flattened-oval, and elongated-oval. By comparing the anteroposterior diameter (APD) (normal group>large group>small group), mediolateral diameter (MLD) (large group>small group>normal group), and APD/MLD ratios among these groups, the condyle of the normal angle group is considered to have an oval shape. The smallest APD was observed in the small angle group, indicating a flattened-oval shape. The large angle group exhibited a longer MLD, higher APD/MLD ratio and AMA, demonstrating an elongated oval condylar shape. (Table 2). The indexes associated with condyle size exhibited a positive correlation with interincisal angle, and the values of the normal angle group fell within the intermediate range. The condylar area and cancellous bone of the small angle group were smaller compared to the normal angle group, while those of the large angle group were larger ($P<0.05$). There is a significant difference between small and large angle groups. The large angle group had a larger condylar size compared to the other two groups, with a larger condylar perimeter, cortical bone area and cancellous/cortical bone area ratio, although there was no statistical difference. The condylar neck angle was larger in both the small and large angle groups when compared to the normal angle group, with the largest value being observed in the large angle group ($P<0.05$). These indicate a more pronounced constriction of the condylar neck in the large angle group. The large angle group exhibited a greater condylar height. As the interincisal angle increases, the mediolateral diameter, AMA, and area of maximum axial condylar and cortical bone tend to increase ($P<0.05$) (Annexed Table 2).

Condylar trabecular bone structure

On the axial plane, the anterior cortical bone was the thickest, followed by the medial, lateral and posterior cortical bones in descending order of thickness (Table 3). In the large angle group, the medial cortical bone was the thinnest while the anterior cortical bone was the thickest. There was no significant difference in cortical bone thickness on the coronal plane among the groups. As the cortical bone thickness on the coronal plane did not follow a normal distribution, a nonparametric test was used. BS and BV exhibited a positive correlation with the interincisal angle, and the values of the normal angle group fell within the intermediate range. The large angle group exhibited significantly higher BS and BV than the small angle group. Small and large angle groups had thinner

Table 2 Statistical analysis of condylar morphology among the three groups. ($n=100$)($\overline{x} \pm s$)

Measurement	Normal angle group	Small angle group	Large angle group	*P*(sig.)		
				P_1	P_2	P_3
APD/ mm	8.47 ± 0.99	8.16 ± 1.00	8.46 ± 1.07	0.032*	0.964	0.035*
MLD/ mm	18.00 ± 1.86	18.10 ± 2.47	18.67 ± 2.09	0.994	0.050	0.178
APD/MLD	2.15 ± 0.33	2.20 ± 0.50	2.23 ± 0.29	0.404	0.261	0.9999
AMA/ degrees	90.10 ± 1.33	90.26 ± 1.42	90.17 ± 1.08	0.364	0718	0.585
The area of maximum condylar axial section/ mm^2	126.00 ± 18.44	123.42 ± 22.81	131.55 ± 25.75	0.130	0.431	0.020*
The area of the maximum axial section of condylar cancellous bone/ mm^2	74.47 ± 14.36	71.40 ± 18.35	78.20 ± 21.75	0.406	0.395	0.043*
The area of the maximum axial section of condylar cortical bone/ mm^2	51.53 ± 7.23	50.98 ± 10.46	53.35 ± 7.49	0.559	0.083	0.249
The ratio of cancellous/cortical bone area	1.46 ± 0.27	1.35 ± 0.37	1.47 ± 0.37	0.172	0.982	0.155
The perimeter of maximum condylar axial section /mm	45.44 ± 4.05	45.56 ± 5.19	46.63 ± 4.72	0.701	0.075	0.161
The perimeter of the maximum axial section of condylar cancellous bone /mm	37.97 ± 4.25	38.01 ± 5.55	39.57 ± 5.12	0.988	0.027*	0.124
The ratio of cancellous bone to cortical perimeter /mm	1.20 ± 0.05	1.18 ± 0.18	1.18 ± 0.06	0.685	0.050	0.018*
The angle of the condylar neck/ degrees	56.45 ± 11.43	57.91 ± 11.80	60.89 ± 12.09	0.755	0.024*	0.218
Condylar height/mm	17.61 ± 2.54	17.69 ± 2.54	18.17 ± 2.55	0.213	0.730	0.112

P_1 means comparison between small angle group and normal angle group; P_2 means comparison between large angle group and normal angle group; P_3 means comparison between the small angle group and large angle group. * $P<0.05$; ** $P<0.01$

Table 3 Statistical analysis of condylar trabecular bone structure among the three groups. ($n=100$)($\overline{x} \pm s$)

Measurement	Normal angle group	Small angle group	Large angle group	*P*(sig.)		
				P_1	P_2	P_3
Anterior cortical bone on the axial plane/mm	1.66 ± 0.44	1.62 ± 0.34	1.67 ± 0.28	0.175	0.015*	0.269
Posterior cortical bone on the axial plane/mm	1.14 ± 0.22	1.15 ± 0.19	1.15 ± 0.17	0.585	0.585	0.585
Medial cortical bone on the axial plane/mm	1.40 ± 0.43	1.45 ± 0.41	1.33 ± 0.32	0.047*	0.047*	0.047*
Lateral cortical bone on the axial plane/mm	1.24 ± 0.30	1.33 ± 0.45	1.27 ± 0.43	0.193	0.193	0.193
Medial cortical bone on the coronal plane/mm	1.34 ± 0.21	1.39 ± 0.28	1.38 ± 0.27	0.479	0.479	0.479
Superior cortical bone on the coronal plane/mm	1.31 ± 0.27	1.35 ± 0.28	1.39 ± 0.29	0.384	0.384	0.384
Lateral cortical bone on coronal plane/mm	1.28 ± 0.23	1.34 ± 0.27	1.28 ± 0.30	0.130	0.130	0.130
BS/mm^2	387.85 ± 79.81	379.13 ± 92.63	397.33 ± 93.91	0.565	0.327	0.045*
BV/mm^3	85.01 ± 15.36	80.72 ± 19.14	87.07 ± 22.55	0.424	0.232	0.021*
BS/BV/$1/m^3$	4.60 ± 0.73	4.74 ± 0.65	4.65 ± 0.71	0.110	0.306	0.563
Tb.Th/μm	2.00 ± 0.56	1.88 ± 0.37	1.88 ± 0.37	0.038*	0.033*	0.971
Tb.N	2.52 ± 1.02	2.67 ± 0.85	2.65 ± 1.00	0.116	0.034*	0.903
Tb.Sp/μm	6.44 ± 2.86	6.26 ± 2.63	6.21 ± 2.42	0.986	0.550	0.562

P_1 means comparison between the small angle group and normal angle group; P_2 means comparison between the large angle group and normal angle group; P_3 means comparison between the small angle group and large angle group; * $P<0.05$; ** $P<0.01$

Table 4 Statistical analysis of condylar position and morphology of the glenoid fossa among the three groups. ($n=100$) ($\overline{x} \pm s$)

Measurement	Normal angle group	Small angle group	Large angle group	*P*(sig.)		
				P_1	P_2	P_3
The horizontal angle of condyle/ degrees	22.70 ± 8.26	24.91 ± 7.34	21.50 ± 7.47	0.043*	0.270	0.002**
Bilateral condylar angle/ degrees	134.60 ± 14.81	130.18 ± 13.26	137.01 ± 13.45	0.113	0.386	0.015*
Condylar vertical angle/ degrees	17.04 ± 5.92	16.34 ± 7.49	14.56 ± 6.83	0.447	0.001**	0.011*
AJS/ mm	2.11 ± 0.61	2.11 ± 0.65	2.20 ± 0.70	0.983	0.354	0.343
SJS / mm	2.24 ± 0.57	2.34 ± 0.65	2.33 ± 0.61	0.246	0.291	0.918
PJS / mm	2.32 ± 0.60	2.45 ± 0.70	2.40 ± 0.52	0.128	0.387	0.511
CCA/ degrees	101.59 ± 6.66	101.75 ± 7.96	98.17 ± 8.70	0.889	0.002*	0.001*
GFW /mm	19.89 ± 1.99	19.48 ± 1.76	20.01 ± 1.86	0.121	0.665	0.048*
GFH /mm	8.37 ± 1.17	8.44 ± 1.81	8.82 ± 1.25	0.867	0.014*	0.009*
GFW/ GFH	0.42 ± 0.05	0.50 ± 0.12	0.44 ± 0.06	0.000001**	0.052	0.000001**
GFA / degrees	111.06 ± 7.62	111.27 ± 8.20	108.65 ± 7.06	0.815	0.029*	0.016*
AEI/ degrees	52.56 ± 10.87	54.17 ± 11.02	59.63 ± 10.38	0.289	0.0001**	0.0001**

P_1 means the comparison between the small angle group and the normal angle group; P_2 means the comparison between the large angle group and the normal angle group; P_3 means the comparison between the small angle group and the large angle group; * $P<0.05$; ** $P<0.01$

Tb.Th and greater Tb.N. Additionally, the Tb.N in the large angle group was greater than that in the normal angle group ($P<0.05$). There was no significant difference in BS/BV and Tb.Sp among the groups, but BS/BV were larger and Tb.Sp were smaller in the small and large angle groups.

Condylar position

There were no significant differences in AJS, SJS, and PJS among the three groups in the sagittal plane ($P<0.05$) (Table 4), indicating no difference in condylar sagittal position within the glenoid fossa. On the axial plane, as the interincisal angle increased, the condylar horizontal angle decreased and reached its minimum value in the larger group. (r=-0.174) ($P<0.05$) (Annexed Table 4). There is a negative correlation between the bilateral condylar angle and the interincisal angle, with the smallest bilateral condylar angle observed in the small angle group ($P<0.05$). These results suggest that, compared to the normal angle group, both the small and large angle groups exhibited condyle rotation. Compared to the normal angle group, both small and large angle groups had smaller condylar vertical angles on the coronal plane. Among them, the large angle group exhibited the smallest condylar vertical angle. These findings suggest a rotation of the condyle in both small and large angle groups within their respective glenoid fossae. Compared to the normal angle group, both small and large angle groups exhibited condylar rotation in the glenoid fossa on the axial and coronal planes, resulting in a change in its position. On the sagittal plane, the large angle group had the smallest CCA ($P<0.05$), indicating a smaller relative distance between the condyle and coracoid processes as the interincisal angle increased.

Morphology of the glenoid fossa

The GFW of the normal angle group fell within the intermediate range, while the small angle group had the smallest GFW and the large angle group had the greatest GFW. Compared to the normal angle group, both small and large angle groups exhibited significantly larger GFH and higher GFW/GFH ratios ($P<0.05$) (Table 4). The small angle group had the highest GFA, whereas the large angle group had the lowest GFA. The small angle group showed a narrower GFW and a higher GFW/GFH ratio, resembling a short cone-shaped glenoid fossa. On the other hand, the large angle group displayed a smaller GFA and a larger GFH, resembling a long cone-shaped glenoid fossa. The AEI of the small angle group and large angle group were higher than that of the normal angle group, with the large angle group having the highest AEI. ($P<0.05$), indicating a steeper posterior articular eminence inclination in this group. The GFH, GFA and AEI tend to increase as the interincisal angle increased, while the GFW/GFH decreased ($P<0.05$) (Annexed Table 5).

Discussion

This study focuses on Angle Class II malocclusion, which has a high incidence. The labial or lingual inclination of the anterior teeth may impact the shape and position of the condyle. The present investigation aims to explore the characteristics of TMJ morphology and position, as well as trabecular structure in individuals with Angle Class II, and examine the correlation between interincisal angle and TMJ morphology, position, and trabecular structure. The sample selection in our study was rigorous, with participants aged 18–35 years who had no mandibular deviation, a skeletal class II type, and a normodivergent facial type [18]. Our findings revealed no significant differences in bilateral morphology, trabecular bone structure, or condyle position ($P>0.05$), indicating that the impact of sample selection on TMJ has been eliminated and both sides of the TMJ were symmetrical.

Condylar size and morphology can be remodelled in different types of dental and maxillofacial malocclusions [19–22]. The condylar size was smallest in Class II compared to Class I and Class III malocclusion [19,23]. The condylar size differed in Class II with different vertical facial types [12]. We focus on the TMJ characteristics of Class II samples (normodivergent facial type) with different interincisal angles. The condylar size was smallest in the small angle group, while it was largest in the large angle group (large group > normal group > small group). The normal angle group exhibited the largest APD (normal group > large group > small group), which is consistent with the findings of the previous study [19]. MLD was largest in the large angle group (large group > small group > normal group). Based on the indexes of APD, MLD and APD/MLD ratios, the normal angle group referred to an oval shape, while the small group had a flattened-oval shape and the large angle group had an elongated-oval shape. Therefore, condyle size and shape varied among sample groups. From the previous study, the anterior occlusal relationship may influence the trabecular bone structure of the condyle [6]. Our findings indicate that there was an increase in Tb.N for small and large angle groups, while Tb.Th exhibited a slight decrease. The reduction in Tb.Th and Tb.Sp may represent compensatory adaptations of the condylar trabecular structure.

The condylar position is influenced by sagittal and vertical skeletal facial types, occlusal relationships, as well as various functional loads [24–26]. The condyle demonstrates rotational movement in both the coronal and horizontal planes, with small and large angles compared to the normal group (Table 4), which is a similar phenomenon observed by Fan [9]. Joint space serves as a commonly used indicator for evaluating the sagittal positioning of the condyle. However, there were no significant variations in joint space among the three groups. Subsequently, another study also observed no statistically significant variation in joint space in class II malocclusion [27]. However, it also has been reported that individuals with Angle II^{1} tend to have a narrower anterior joint space compared to those with Angle $II^{[2\ [8{\cdot}28]]}$. This discrepancy may be attributed to the lack of specification regarding vertical facial types in the aforementioned studies.

The size and shape of the condyle can modify stress distribution within the glenoid fossa, thereby inducing remodelling of the fossa [29,30]. The condyle is larger and the glenoid fossa is deeper and wider in the large-angle group. The morphology of the glenoid fossa in the large angle group resembles a long cone shape, while both the normal and small angle groups resemble a short cone. As reported before, Class II^{1} exhibited a greater width and depth in the glenoid fossa compared to Class $II^{[2\ [19]]}$. The condyle and glenoid fossa exhibit a close structural relationship that affects their functional interdependence [19].

This study revealed the condylar morphology, trabecular bone structure, and glenoid fossa morphology of the TMJ in Angle Class II malocclusions. Previous knowledge regarding the association between interincisal angle and TMJ was limited. The interincisal angle serves as a clinically accessible index, and this study has demonstrated its correlation with condylar morphology, trabecular bone structure, and glenoid fossa morphology. A comprehensive understanding of its connection to the TMJ is crucial for formulating effective treatment plans. Restoring normal interincisal angles through orthodontic treatment can establish a favourable environment for TMJ function, while achieving proper interincisal angles

contributes to maintaining dental stability and optimal occlusal contact, thereby facilitating masticatory function and reducing the risk of relapse. However, there are limitations to this study, such as the absence of male samples. Subsequent studies aiming to comprehensively assess the impact of the interincisal angle on TMJ would require additional male samples. Currently, research on the interincisal angle remains incomplete; nevertheless, exploring its relationship with TMJ is worthwhile. In future investigations, a larger sample size could be included to explore how the interincisal angle influences both morphological characteristics and microstructure of TMJ in populations with vertical or sagittal skeletal types.

Conclusion

This paper presents a summary of the TMJ characteristics observed in Angle Class II malocclusion. Interincisal angle exerts an influence on the morphology/position and trabecular structure of the TMJ. When the interincisal angle exceeds the normal range, the TMJ undergoes a series of changes. Individuals with a smaller interincisal angle may exhibit a flattened-oval shape and larger condyles, wider and shallower glenoid fossae, and lower Tb.Th and higher Th.N, and sharper articular eminences. Conversely, an excessively large interincisal angle exhibited elongated oval condyles and increased condylar sizes, lower Tb.Th and higher Th.N, deeper glenoid fossae, and more pronounced articular eminences. In individuals with smaller or larger interincisal angles, the condyle rotates within the glenoid fossa on both the axial and coronal planes compared to those with a normal interincisal angle. This implies that we must pay attention to the relationship between the interincisal angle and TMJ, and it is crucial to restore the normal interincisal angle during orthodontic treatment.

Supplementary Information

The online version contains supplementary material available at https://doi.org/10.1186/s12903-024-04788-4.

Supplementary Material 1

Acknowledgements
Not applicable.

Author contributions
Liangjiao Chen designed the research. Xiaowen Hu was responsible for the measurement, and data analysis and drafted the manuscript. Data curation was performed by Ziwei Chen. The project administration and funding acquisition were performed by Minhua Mo and Xiaohe Zhou. All authors read, corrected, and approved the manuscript.

Funding
This work was supported financially by the National Natural Science Fund (No.81600904) and the Open Laboratory Project for College Students of Guangzhou Medical University (No. 20205028).

Data availability
The data supporting the findings of this study are not openly available due to sensitivity reasons and can be obtained from the corresponding author upon reasonable request. The data is stored in a controlled access data storage at Stomatological Hospital affiliated to Guangzhou Medical University.

Declarations

Ethics approval and consent to participate
This study was approved by the Research Ethics Committee of Stomatological Hospital affiliated with Guangzhou Medical University (No. LCY2022019). The informed consent of all patients, as well as their legal guardians or representatives, was obtained before participation. We affirm that all methods were conducted in accordance with relevant guidelines and regulations.

Consent for publication
Not applicable.

Competing interests
The authors declare no competing interests.

Author details
[1]Department of Orthodontics, Guangdong Engineering Research Center of Oral Restoration and Reconstruction, Guangzhou Key Laboratory of Basic and Applied Research of Oral Regenerative Medicine, Affiliated Stomatology Hospital of Guangzhou Medical University, Guangzhou 510182, Guangdong, People's Republic of China

Received: 23 January 2024 / Accepted: 21 August 2024
Published online: 30 August 2024

References

1. Stocum DL, Roberts WE, Part I. Development and physiology of the Temporomandibular Joint. Curr Osteoporos Rep. 2018;16:360–8.
2. Kurusu A, Horiuchi M, Soma K. Relationship between occlusal force and mandibular condyle morphology. Evaluated by limited cone-beam computed tomography. Angle Orthod. 2009;79:1063–9.
3. Burke G, Major P, Glover K, Prasad N. Correlations between condylar characteristics and facial morphology in Class II preadolescent patients. Am J Orthod Dentofac Orthop. 1998;114:328–36.
4. Yale SH, Allison BD, Hauptfuehrer JD. An epidemiological assessment of mandibular condyle morphology. Oral Surg Oral Med Oral Pathol. 1966;21:169–77.
5. Wohlberg V, Schwahn C, Gesch D, Meyer G, Kocher T, Bernhardt O. The association between anterior crossbite, deep bite and temporomandibular joint morphology validated by magnetic resonance imaging in an adult non-patient group. Ann Anat. 2012;194:339–44.
6. Choi DY, Sun KH, Won SY, Lee JG, Hu KS, Kim KD, et al. The trabecular bone ratio of the mandibular condyle according to the presence of teeth: a micro-CT study. Surg Radiol Anat. 2012;34:519–26.
7. Al-Khateeb EA, Al-Khateeb SN. Anteroposterior and vertical components of class II division 1 and division 2 malocclusion. Angle Orthod. 2009;79:859–66.
8. Gorucu-Coskuner H, Ciger S. Computed tomography assessment of temporomandibular joint position and dimensions in patients with class II division 1 and division 2 malocclusions. J Clin Exp Dent. 2017;9:e417–23.
9. Fan XC, Ma LS, Chen L, Singh D, Rausch-Fan X, Huang XF. Temporomandibular Joint Osseous morphology of class I and Class II malocclusions in the normal skeletal pattern: a Cone-Beam Computed Tomography Study. Diagnostics (Basel). 2021;11.
10. Alhammadi MS. Dimensional and positional characteristics of the Temporomandibular Joint of skeletal class II malocclusion with and without Temporomandibular disorders. J Contemp Dent Pract. 2022;23:1203–10.
11. Thompson JR. Abnormal function of the temporomandibular joints and related musculature. Orthodontic implications. Part II. Angle Orthod. 1986;56:181–95.
12. Lin M, Xu Y, Wu H, Zhang H, Wang S, Qi K. Comparative cone-beam computed tomography evaluation of temporomandibular joint position and morphology in female patients with skeletal class II malocclusion. J Int Med Res. 2020;48:300060519892388.

13. Mao B, Tian Y, Wang X, Li J, Zhou Y. [Soft and hard tissue changes of hyperdivergent class II patients before and after orthodontic extraction treatment]. Beijing Da Xue Xue Bao Yi Xue Ban. 2024;56:111–9.
14. Thiesen G, Gribel BF, Freitas MPM, Oliver DR, Kim KB. Mandibular asymmetries and associated factors in orthodontic and orthognathic surgery patients. Angle Orthod. 2018;88:545–51.
15. Domander R, Felder AA, Doube M. BoneJ2 - refactoring established research software. Wellcome Open Res. 2021;6:37.
16. Lo Giudice A, Rustico L, Caprioglio A, Migliorati M, Nucera R. Evaluation of condylar cortical bone thickness in patient groups with different vertical facial dimensions using cone-beam computed tomography. Odontology. 2020;108:669–75.
17. Hasebe A, Yamaguchi T, Nakawaki T, Hikita Y, Katayama K, Maki K. Comparison of condylar size among different anteroposterior and vertical skeletal patterns using cone-beam computed tomography. Angle Orthod. 2019;89:306–11.
18. Liu Q, Wei X, Guan J, Wang R, Zou D, Yu L. Assessment of condylar morphology and position using MSCT in an Asian population. Clin Oral Investig. 2018;22:2653–61.
19. Song J, Cheng M, Qian Y, Chu F. Cone-beam CT evaluation of temporomandibular joint in permanent dentition according to Angle's classification. #N/A. 2019;36:261–6.
20. Lobo F, Tolentino ES, Iwaki LCV, Walewski LA, Takeshita WM, Chicarelli M. Imaginology Tridimensional Study of Temporomandibular Joint Osseous Components according to Sagittal Skeletal Relationship, sex, and Age. J Craniofac Surg. 2019;30:1462–5.
21. Kuroda S, Tanimoto K, Izawa T, Fujihara S, Koolstra JH, Tanaka E. Biomechanical and biochemical characteristics of the mandibular condylar cartilage. Osteoarthritis Cartilage. 2009;17:1408–15.
22. Meikle MC. Remodeling the dentofacial skeleton: the biological basis of orthodontics and dentofacial orthopedics. J Dent Res. 2007;86:12–24.
23. Saccucci M, D'Attilio M, Rodolfino D, Festa F, Polimeni A, Tecco S. Condylar volume and condylar area in class I, class II and class III young adult subjects. Head Face Med. 2012;8:34.
24. Paknahad M, Shahidi S. Association between condylar position and vertical skeletal craniofacial morphology: a cone beam computed tomography study. Int Orthod. 2017;15:740–51.
25. Paknahad M, Shahidi S, Abbaszade H. Correlation between condylar position and different sagittal skeletal facial types. J Orofac Orthop. 2016;77:350–6.
26. Almaqrami BS, Alhammadi MS, Tang B, Hua ESAL, He F. Three-dimensional morphological and positional analysis of the temporomandibular joint in adults with posterior crossbite: a cross-sectional comparative study. J Oral Rehabil. 2021;48:666–77.
27. Gianelly AA, Petras JC, Boffa J. Condylar position and class II deep-bite, no-overjet malocclusions. Am J Orthod Dentofac Orthop. 1989;96:428–32.
28. Katsavrias EG, Halazonetis DJ. Condyle and fossa shape in Class II and Class III skeletal patterns: a morphometric tomographic study. Am J Orthod Dentofac Orthop. 2005;128:337–46.
29. İlgüy D, İlgüy M, Fişekçioğlu E, Dölekoğlu S, Ersan N. Articular eminence inclination, height, and condyle morphology on cone beam computed tomography. ScientificWorldJournal. 2014;2014:761714.
30. Honda K, Larheim TA, Sano T, Hashimoto K, Shinoda K, Westesson PL. Thickening of the glenoid fossa in osteoarthritis of the temporomandibular joint. An autopsy study. #N/A. 2001;30:10–3.

Publisher's note

Springer Nature remains neutral with regard to jurisdictional claims in published maps and institutional affiliations.